An astral simulacrum of the central spindle accounts for normal, spindle-less, and anucleate cytokinesis in echinoderm embryos

Kuan-Chung Su[a,b,*,†], William M. Bement[a,c], Mark Petronczki[b], and George von Dassow[a,*]
[a]Oregon Institute of Marine Biology, Charleston, OR 97420; [b]Cancer Research UK London Research Institute, Clare Hall Laboratories, South Mimms EN6 3LD, United Kingdom; [c]Laboratory of Cell and Molecular Biology, University of Wisconsin, Madison, WI 53706

ABSTRACT **Cytokinesis in animal cells depends on spindle-derived spatial cues that culminate in Rho activation, and thereby actomyosin assembly, in a narrow equatorial band. Although the nature, origin, and variety of such cues have long been obscure, one component is certainly the Rho activator Ect2. Here we describe the behavior and function of Ect2 in echinoderm embryos, showing that Ect2 migrates from spindle midzone to astral microtubules in anaphase and that Ect2 shapes the pattern of Rho activation in incipient furrows. Our key finding is that Ect2 and its binding partner Cyk4 accumulate not only at normal furrows, but also at furrows that form in the absence of associated spindle, midzone, or chromosomes. In all these cases, the cell assembles essentially the same cytokinetic signaling ensemble—opposed astral microtubules decorated with Ect2 and Cyk4. We conclude that if multiple signals contribute to furrow induction in echinoderm embryos, they likely converge on the same signaling ensemble on an analogous cytoskeletal scaffold.**

Monitoring Editor
Thomas D. Pollard
Yale University

Received: Apr 4, 2014
Revised: Sep 11, 2014
Accepted: Oct 1, 2014

INTRODUCTION

All eukaryotes need to coordinate nuclear division, whether mitosis or meiosis, with partitioning of the cytoplasm—cytokinesis. In animal cells, cytokinetic apparatus assembly depends on spatial information provided by the mitotic apparatus at the end of M phase (reviewed by Green *et al.*, 2012). Without such information, cortical contractility develops everywhere or not at all (Canman *et al.*, 2000; Foe and von Dassow, 2008). Classical experiments, primarily on large cells of marine invertebrate embryos, showed that the astral microtubule arrays extending from each spindle pole suffice to correctly localize the division plane (reviewed by Rappaport, 1996). In small cells, however, analogous experiments show that the relevant spatial cue emanates from the midzone of the mitotic apparatus (e.g., Cao and Wang, 1996). This conclusion is strongly supported by genetic analysis of cytokinesis in diverse organisms, including embryonic cells such as *Caenorhabditis elegans* zygotes, because midzone-associated gene products, such as the centralspindlin complex, are consistently implicated in the control of cytokinetic apparatus assembly and function (reviewed by White and Glotzer, 2012; Green *et al.*, 2012).

To reconcile classical and recent results, one might argue that cells use two or more distinct, and normally redundant, patterning mechanisms that converge upon the same result, or that the overlap of astral microtubules at the cell equator replicates the structural conditions at the spindle midzone (such that only one mechanism is in fact at work), or that one or another set of results is wrong or otherwise misleading. To dispel the last possibility, in previous work ,we replicated key experiments on echinoderm embryonic cells to demonstrate, using a fluorescent microtubule probe, that cells can cleave without a spindle or without astral microtubules but cleave inaccurately when one aster is diminished relative to the other (von Dassow *et al.*, 2009). From these facts, we argued that in the large cells of early echinoderm embryos, the spindle midzone must be a source of a diffusible signal, which, under normal conditions, is spatially focused in the equator by astral microtubules.

This article was published online ahead of print in MBoC in Press (http://www.molbiolcell.org/cgi/doi/10.1091/mbc.E14-04-0859) on October 8, 2014.

*These authors contributed equally.

†Present address: Whitehead Institute for Biomedical Research and Department of Biology, Massachusetts Institute of Technology, Cambridge, MA 02142.

Address correspondence to: George von Dassow (dassow@uoregon.edu).

Abbreviations used: EMTB, ensconsin microtubule-binding domain; FSW, filtered seawater; GEF, guanine nucleotide exchange factor; rGBD, rhotekin GTPase-binding domain; wt, wild type.

© 2014 Su *et al*. This article is distributed by The American Society for Cell Biology under license from the author(s). Two months after publication it is available to the public under an Attribution–Noncommercial–Share Alike 3.0 Unported Creative Commons License (http://creativecommons.org/licenses/by-nc-sa/3.0).

"ASCB®," "The American Society for Cell Biology®," and "Molecular Biology of the Cell®" are registered trademarks of The American Society for Cell Biology.

Candidates for such a diffusible signal include the centralspindlin complex, because it localizes to the spindle midzone in a wide variety of cleaving animal cells, its motor activity suggests an obvious mechanism for focusing by astral microtubules, and it interacts directly with the cell membrane (Nislow *et al.*, 1992; Adams *et al.*, 1998; Mishima *et al.*, 2002; Hutterer *et al.*, 2009; Lekomtsev *et al.*, 2012); or its direct interactor, Ect2, a guanine nucleotide exchange factor (GEF) for Rho-family GTPases that is essential for cytokinesis in animal cells (Prokopenko *et al.*, 1999; Tatsumoto *et al.*, 1999; Somers and Saint, 2003; Yüce *et al.*, 2005); even active Rho itself, whose activity at the equatorial cortex constitutes the "cut along dotted line" for animal cells (Bement *et al.*, 2005); or some other factor, such as the chromosome passenger complex, which has been shown to move from midzone to equator during cytokinesis (Eckley *et al.*, 1997; Murata-Hori and Wang, 2002).

Previous work in culture human cells showed that Ect2 accumulates not only at the spindle midzone, but also in an equatorial cortical gradient during cytokinesis in cultured mammalian cells (Chalamalasetty *et al.*, 2006; Su *et al.*, 2011). In such cells, there is little difficulty envisioning how a midzone-derived signal might cross the modest gap between spindle and cortex. However, the homologous gap in large cells of early embryos is tens or hundreds of micrometers across. Nevertheless, we report here that in sea urchins and starfish embryos, Ect2 exhibits all the behaviors and activities required to fulfill the role of the signal that transmutes spindle position into patterned Rho activation at the cell equator. Although its localization in echinoderm embryonic cells is slightly different from that in cultured mammalian cells, we find that Ect2 recruits to the midzone in anaphase, then with astral microtubules reaching up to the equator. We show that Ect2 potently shapes the pattern of Rho activation. Finally, we demonstrate that Ect2 (along with centralspindlin) is present beneath cleavage furrows that form between juxtaposed asters.

RESULTS

Ect2 recruits to the central spindle and astral microtubules

To visualize Ect2 in early embryos, we fused purple urchin Ect2 (SpEct2) to 3x enhanced green fluorescent protein (eGFP; Figure 1A). When injected as mRNA into urchin or sand dollar zygotes at levels typically used for other probes, wild-type Ect2 caused overt defects as early as first cleavage (see later discussion). At much lower doses, however, embryos developed normally, and we could detect changing localization of Ect2 throughout the cell cycle as early as the eight-cell stage (Figure 1B, Supplemental Figure S1A, and Supplemental Video S1). As in other animal cells, Ect2 was nuclear during interphase, dispersed cytoplasmically in metaphase, and appeared on the central spindle just after anaphase onset. As anaphase progressed, we observed faint signal in the cytoplasmic disk between the central spindle and the equatorial cortex (Figure 1B and Supplemental Video S1). Although Ect2 did associate with the cell cortex in embryos during anaphase, especially when expressed at high levels, and we occasionally detected cortical enrichment in incipient furrows (Figure 1B′), we did not consistently observe a gradient of Ect2 at the equatorial membrane, as described in mammalian cells, in early embryos. By the blastula stage, however, once cells achieved the same scale as typical cultured somatic cells, we frequently observed equatorial cortical enrichment similar to mammalian cells (Supplemental Figure S1B). This distinction may, in principle, reflect detectability rather than actual presence or absence of an Ect2 gradient in the equatorial cortex. However, early embryonic cells that did exhibit clear cortical Ect2 also tended to exhibit abnormal behavior (described later), suggesting that the apparent difference between small and large cells is real: large cells lack the cortical gradient; midzone and the aster overlap region account for the bulk of localized Ect2.

Urchin and sand dollar embryos proved acutely sensitive to increasing doses of wild-type Ect2, exhibiting cortical hypercontractility and blebbing, or even outright cleavage failure, as early as the first division (Figure 2, A and B, and Supplemental Video S4). To improve visualization of Ect2 without inducing ectopic contractions, we mutated the GEF domain (Figure 1A). SpEct2 GEF4A (as in Su *et al.*, 2011) was tolerated at higher levels than wild-type (wt) Ect2 and exhibited similar localization (Figure 1C and Supplemental Figure S1D), although it behaves as an apparent dominant negative when expressed at high levels (see later discussion) and did not associate with the cortex as much as wt Ect2 (Figure 3). Ect2 GEF4A thus gave us a much clearer view of Ect2 association with overlapping astral microtubules in the region between the central spindle and the equatorial cortex (Figure 1C and Supplemental Videos S2 and S3); at levels sufficient to inhibit cleavage, Ect2 GEF4A appeared to stream along astral microtubules, accumulating at intersections between asters (Figure 3 and Supplemental Video S5).

We took advantage of the fact that starfish oocytes can be cultured after injection for several days before fertilization to allow wt 3xGFP Ect2 to accumulate to visible levels in time for first cleavage. Despite mild cortical hyperactivity, starfish embryos better tolerated extra wt Ect2 while displaying identical localization as in urchins (Figure 4A and Supplemental Video S6). As in urchin embryos, we saw little evidence of an Ect2 gradient in the nascent furrow (unless Ect2 was expressed at pathological levels) until the early blastula stage. On the other hand, Ect2 was clearly detectable on astral microtubules even in the earliest divisions: coexpression of wt 3xGFP Ect2 with 2xmCh ensconsin microtubule-binding domain (EMTB) showed that Ect2 associated with distal portions of equatorially directed astral microtubules beginning in anaphase. Ect2-decorated astral microtubules reached progressively further toward the cortex and then became brighter as they were collected by the ingressing furrow (Figure 4, A′ and A″). Kymographs of the equatorial region illustrate redistribution of Ect2 from central spindle to the asters to the membrane over time as the furrow constricts (Figure 4B and Supplemental Figure S1D).

Ect2 activity might, in principle, be required for patterned Rho activation during cytokinesis but nevertheless not be the primary determinant for that pattern. Similarly, Ect2 activity might be required to sustain, but not initiate, furrowing. For Ect2 localization to account for the initial position of the cytokinetic furrow, it must be nonuniformly distributed in relation to the equatorial cortex before overt furrowing begins. It proved challenging to determine whether this is so in early embryos, because any clearly visualizable level of wild-type Ect2 elicited abnormal cortical behavior, implying that an excess was present. However, analysis of two other features is strongly suggestive. First, when present in slight excess (i.e., in cells that cleave accurately but display ectopic cortical contractility during cleavage), wild-type Ect2 accumulates in a rind throughout the cortex during anaphase (Supplemental Figures S1A and S2A); this rind develops 1–3 min before furrow initiation, regardless of cell size or species. This suggests that Ect2 acquires the ability to associate with the cortex during anaphase. Second, we used kymographic analysis of cells expressing 3xGFP Ect2 GEF4A to assess the relative time at which the astral "ladder" of Ect2-decorated microtubules reaches from midzone to equatorial surface (Supplemental Figure S2C); the ladder spanned the entire radius of the cell concurrent with or slightly before furrow initiation.

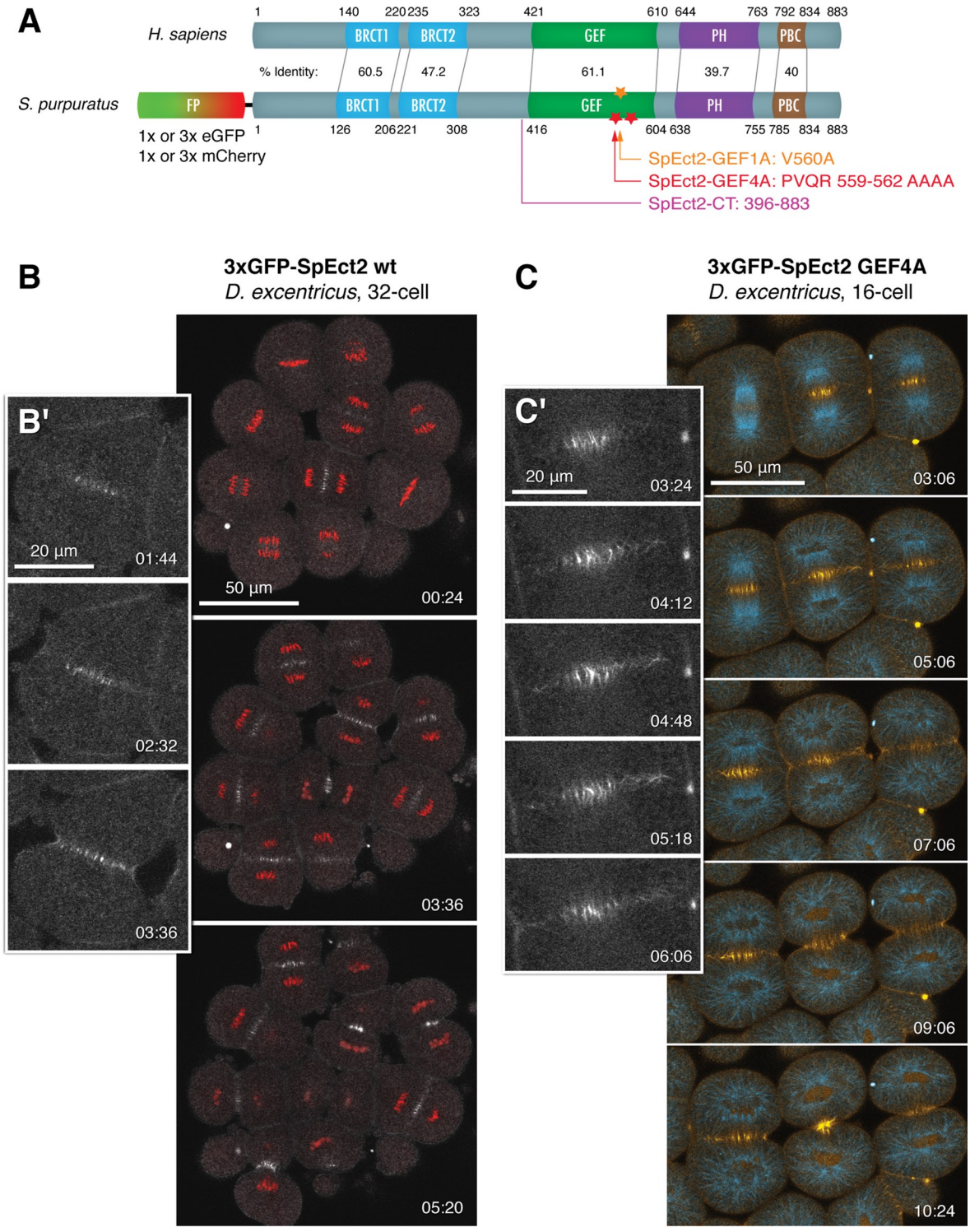

FIGURE 1: Urchin Ect2 recruits to the central spindle and the astral microtubule ladder. (A) Schematic of urchin vs. human Ect2, showing positions of tags and derivatives used. (B) Wild-type 3xGFP Ect2 (gray) in 32-cell sand dollar coexpressed with mCh-H2B (red); single optical sections (Supplemental Video S1). (B′) Two-times magnification of the indicated cell immediately before, early in, and mid cleavage. (C) 3xGFP Ect2 GEF4A (gold) in 16-cell sand dollar embryo coexpressed with 2xmCh EMTB (cyan; Supplemental Video S2). (C′) Two-times magnification of the middle cell during the period when the astral ladder develops between central spindle and equatorial cortex.

To relate Ect2 localization to that of its binding partner Cyk4/MgcRacGAP (a member of the centralspindlin complex), we expressed 3xGFP SpCyk4 in starfish oocytes. As in other animal cells (reviewed by White and Glotzer, 2012), SpCyk4 recruited to the central spindle immediately after anaphase onset; shortly thereafter, Cyk4 was faintly detectable on astral microtubules throughout the cytoplasm and then accumulated on equatorially directed astral microtubules, reaching the cortex concomitant to furrow initiation and

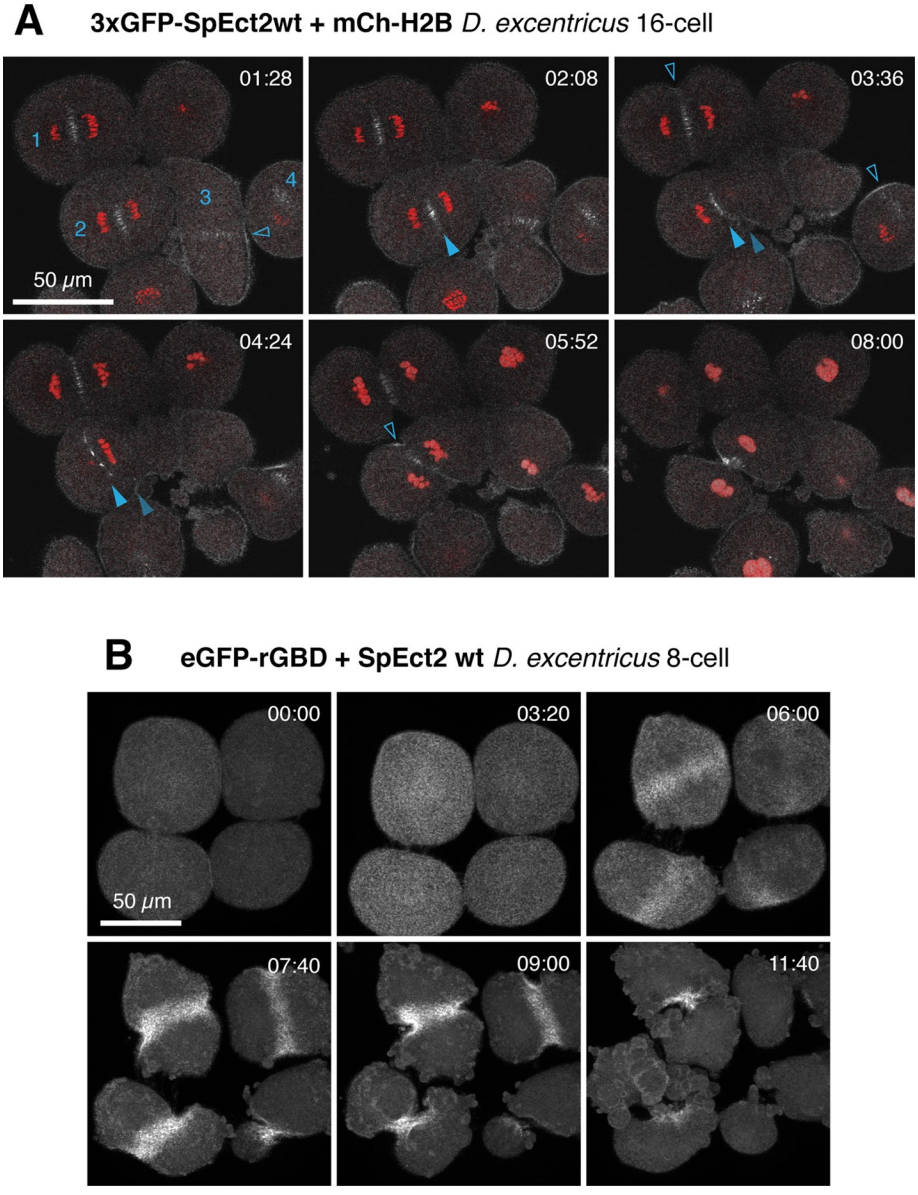

FIGURE 2: Wild-type Ect2 induces hypercontractility during cytokinesis. (A) Sand dollar embryo expressing 3xGFP SpEct2 WT(white) and mCh-H2B (red), single section. Cells 1–4 exhibit various behaviors, likely due to variation in the amount of Ect2 mRNA inherited after injection: cell 1 cleaves normally, and cells 2–4 are hyperactive. Open arrowheads point out instances of cortical Ect2; solid arrowheads follow the midzone in cell 2 as it slips when the cell contracts. See Supplemental Video S4. (B) Eight-cell sand dollar embryo coexpressing eGFP-rGBD and wt SpEct2, projection of 15 1-μm sections; these cells exhibit broad furrow zones and ectopic Rho activation. Times are minutes:seconds after filming began.

remaining associated with astral microtubules gathered by the furrow into the midbody (Figure 4C and Supplemental Video S7). Based on these results and the known binding of Ect2 and Cyk4 (Somers and Saint, 2003; Yüce *et al.*, 2005), it seems likely that centralspindlin recruits Ect2 to astral microtubules in the disk of cytoplasm beneath the equator and the incipient furrow region.

Ect2 shapes the cytokinetic Rho zone

Overexpression of wild-type Ect2 in urchins induces ectopic contraction, blebbing, and spindle slippage during furrow ingression (Figure 2), whereas expression of high levels of GEF-dead Ect2 GEF4A inhibits furrowing and cortical contraction, to the point of blocking cytokinesis completely (Figure 3). Because Rho is presumed to be the primary target of Ect2 during cytokinesis, we coexpressed wt or mutant Ect2 with eGFP–rhotekin GTPase–binding domain (rGBD; which detects active Rho specifically) to evaluate the effect of Ect2 on the spatial domain of Rho activation. In these experiments, we were careful to remain within a dosage range for Ect2 that was free of overt cytokinetic defects (such as the blebbing shown in Figure 2B) and at which visible Ect2 is confined to the equator during anaphase. Wt Ect2 induced a dramatically broader and brighter domain of Rho activity (Figure 5A and Supplemental Video S8). Conversely, expression of Ect2 GEF4A reduced the zone of active Rho to the point that it was barely detectable (Figure 5B). These effects were consistent across a range of mRNA dose and cell size (Figure 5, C and D). A milder hypomorphic single mutation of the GEF domain (V560A), which, based on results in other organisms, is expected to significantly reduce but not eliminate GEF activity (Liu *et al.*, 1998; Propopenko *et al.*, 1999; Schumacher *et al.*, 2004), had no measurable effect on the cytokinetic Rho zone at equivalent expression levels. Increasing levels of wt Ect2 (i.e., to the range shown in Figure 2, A and B) also led to ectopic Rho activity outside the furrow zone, whereas excess Ect2 GEF4A prevented furrowing entirely. From these results, we conclude that the spatial pattern of Rho activation at the cell surface is determined directly by the localization and activity of Ect2.

In human cells, a truncation removing the N-terminal region including the BRCT domains (Ect2CT) prevents Ect2 from recruiting to the central spindle and causes it to accumulate at the cell surface (Chalamalasetty *et al.*, 2006; Su *et al.*, 2011). In urchin embryos, the equivalent mutant potently deranged cortical behavior within ½ h of injecting mRNA, causing cells to contract themselves to death. We therefore injected zygotes with eGFP-rGBD mRNA and then injected one of four cells with Ect2CT mRNA. Rho was uniformly activated across the surface of Ect2CT-injected cells. Strikingly, the total cortical rGBD signal intensity in Ect2CT-injected cells vastly exceeded the total signal in the furrows of uninjected neighboring cells (Figure 5E). From this, we conclude that unrestrained and delocalized Ect2 activity abolishes the cytokinetic pattern of Rho activity. Furthermore, this outcome reveals that the amount of Rho activated during normal cytokinesis is a tiny fraction of the available pool.

Ect2 and centralspindlin account for secondary furrows

The apparent dependence of normal furrowing on central spindle–localized proteins, plus the well-documented propensity for diverse

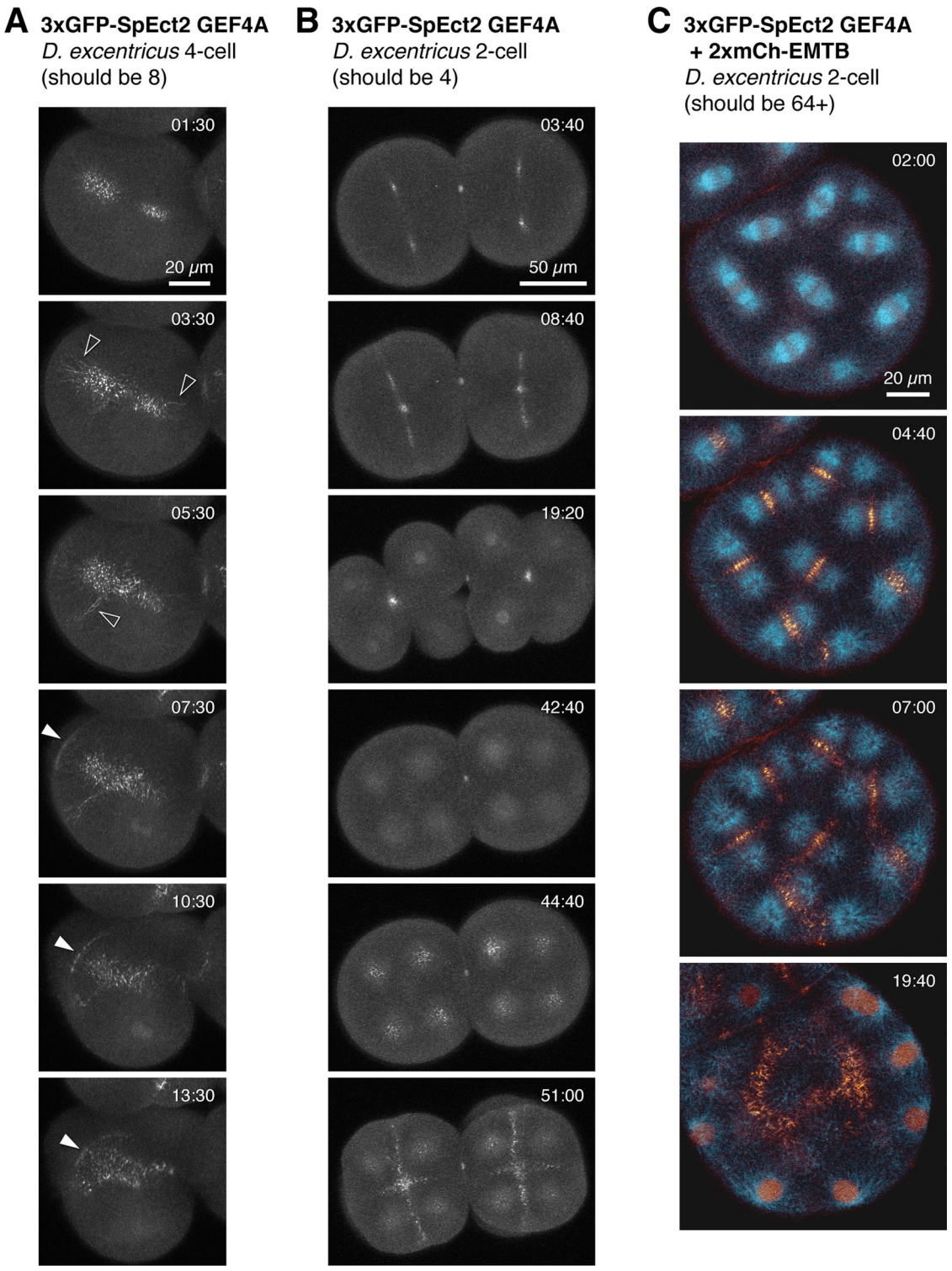

FIGURE 3: Too much Ect2-G4A inhibits furrowing. (A, B), Projections of 16 1-μm (A) or 13 2-μm (B) sections of sand dollar embryos expressing sufficient 3xGFP Ect2 GEF4A to cause cytokinesis failure. Embryos failed cytokinesis once before imaging began. (A) t = 01:30 and (B) t = 44:40 end-on views through the central spindle, where Ect2 accumulates before moving to astral microtubules, indicated by open arrowheads in A. See Supplemental Video S5. Solid arrowheads point out cortical Ect2 in the ingressing furrow. (C) Sand dollar embryo expressing 3xGFP Ect2 GEF4A (gold) and 2xmCh EMTB (blue), which has undergone multiple cycles of cytokinesis failure (18 1-μm sections). As the cell progresses through anaphase, Ect2 relocates from central spindle to overlapping astral microtubule regions, which remain after nuclear reassembly. Times are minutes:seconds after filming began.

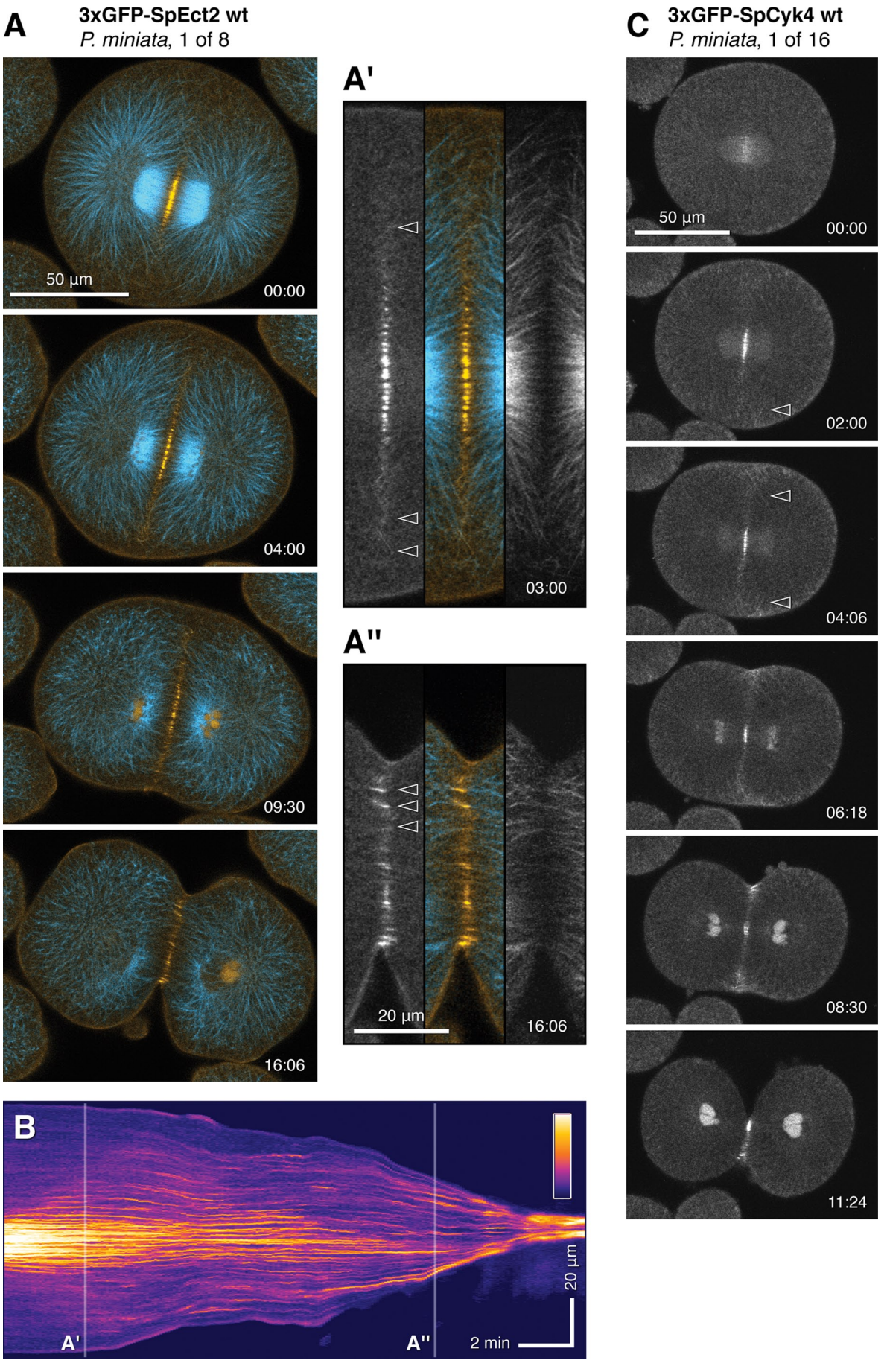
A
3xGFP-SpEct2 wt
P. miniata, 1 of 8
50 µm
00:00
04:00
09:30
16:06
A'
03:00
A"
20 µm
16:06
B
A'
A"
2 min
20 µm
C
3xGFP-SpCyk4 wt
P. miniata, 1 of 16
50 µm
00:00
02:00
04:06
06:18
08:30
11:24

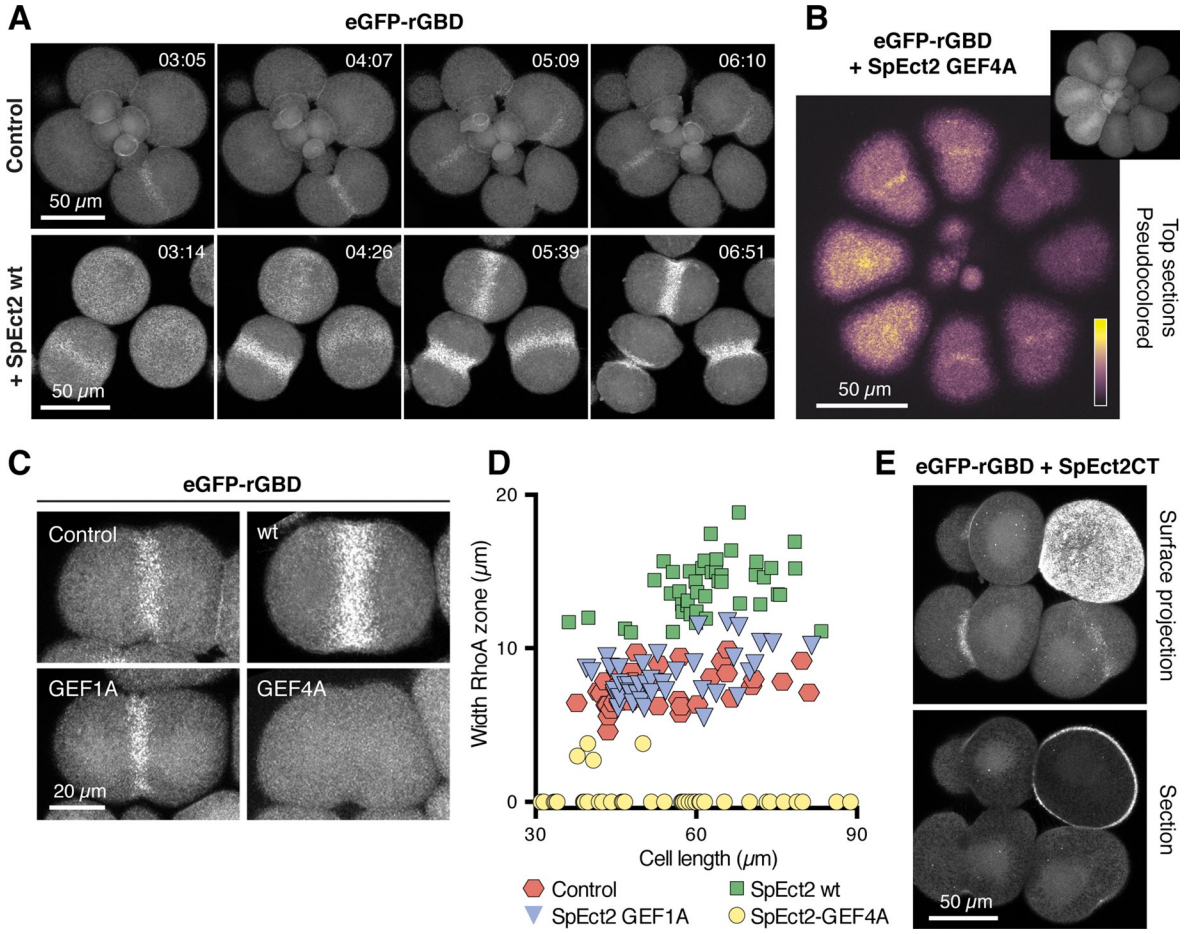

FIGURE 5: Ect2 shapes the zone of active Rho. (A) Comparison of sand dollar embryos at the 16- to 32-cell division, expressing GFP-rGBD alone or with wt Ect2; projections of 15 (control) or 20 (Ect2) 1-μm sections (Supplemental Video S8). The dose of Ect2 used here was low enough that no overt defects were evident, but the embryo displays a broadened, brightened Rho zone. (B) Single surface section of 32-cell sand dollar embryo expressing GFP-rGBD and a dose of SpEct2 GEF4A at which no defects were apparent. False coloring was applied to highlight faint active Rho zones, which are not detectable in a projection of 11 1-μm sections displayed in the inset. (C) Representative projections of single sand dollar cells at equivalent cell sizes at onset of furrowing, injected with GFP-rGBD alone, or with low dose of wt Ect2 and GEF1A or GEF4A mutants. (D) Plot of cell size vs. width of Rho zone from images as in C. (E) Projection of all 28 (top) or four medial (lower) 0.8-μm sections of a dividing four-cell sand dollar embryo expressing eGFP-rGBD. Top right cell was also injected with mRNA encoding hyperactive SpEct2-CT and displays strong Rho activity over the entire surface.

cells to develop furrows between pairs of asters in various experimental circumstances, suggests the possibility that overlapping, mechanistically distinct signals contribute to furrow induction (as in Murata-Hori and Wang, 2002; Bringmann and Hyman, 2005; Baruni *et al.*, 2008; von Dassow, 2009). At least some animal cells, such as *C. elegans* embryos, possess spindle- and centralspindlin-independent means to signal furrow initiation (Dechant and Glotzer, 2003; Werner *et al.*, 2007; Tse *et al.*, 2012). Alternatively, it may be that the same signaling mechanism can interpret diverse geometric arrangements of microtubules into a similar outcome. To test this, we used several approaches to disrupt astral microtubules or separate them physically from the spindle. We showed previously that trichostatin A strongly inhibits astral microtubule growth while leaving the spindle functional for anaphase and that such asterless cells cleave accurately despite a much broader than normal zone of Rho activity (von Dassow *et al.*, 2009). Accordingly, we found that in

FIGURE 4: Ect2 and centralspindlin climb the astral ladder in starfish. (A) One of eight cells in a starfish embryo expressing wt 3xGFP SpEct2 (gold) and 2xmCh EMTB (cyan; Supplemental Video S6). (A′, A″) Two-times magnifications of the region covering central spindle and cell equator before and midway through cleavage, with Ect2 (left), merge (middle), and microtubules (right). Arrowheads in A′ indicate astral microtubules decorated by Ect2. Arrowheads in A″ indicate Ect2-decorated microtubule bundles—the ladder—that cross the equator parallel to the spindle. (B) Kymograph from same sequence as A; times of A′ and A″ shown by vertical lines. Note the diagonal spread of Ect2 from central spindle to cell surface and that the central spindle itself grows dimmer over time as the ladder grows brighter. (C) One of 16 cells in a starfish embryo expressing wt 3xGFP SpCyk4, which appears on the central spindle and faintly on astral rays throughout the cell in anaphase (first frame) and then clears from the spindle poles outward and accumulates on astral microtubules beneath the furrow (Supplemental Video S7).

trichostatin A–treated cells, Ect2 remained concentrated at the central spindle and on tips of short astral microtubules (Figure 6) and was only faintly detectable over a broad region around the equatorial cortex, corresponding to the wider than normal furrow. Cyk4 behaved similarly (unpublished data). This is consistent with the idea that astral microtubules serve to focus a central spindle–derived signal—Ect2—that would otherwise reach the cell surface by diffusion.

We next tested whether Ect2 and centralspindlin are localized to furrows that form between two asters without a spindle between them ("secondary" furrows). The classic instance is the toroidal cell, which, as described originally by Rappaport (1961), first cleaves to make a binucleate, U-shaped cell; at second mitosis, it cleaves from one to four cells with two furrows crossing spindles and one that passes between two asters. We perforated Ect2- or Cyk4-expressing starfish zygotes or blastomeres from the 2- to 16-cell stage with a 40- to 60-μm glass bead. Ect2 consistently appeared, albeit more faintly than in the primary furrows, in the overlap zone where a secondary furrow ingressed, becoming concentrated to a midbody in all cases in which the secondary furrow completed (Figure 7, A and B, and Supplemental Video S9). Cyk4 always recruited robustly to the secondary furrow (Figure 7C and Supplemental Video S10). Of interest, perforated cells expressing Ect2 or Cyk4 also displayed elevated cortical contractility, and occasionally an ingressing furrow, on the far side of the torus during the first mitosis (Supplemental Videos S9 and S10); although we did not unambiguously detect Ect2 in such cases, Cyk4 consistently decorated distal portions of astral microtubules on the far side of the torus, albeit much less well focused than at second mitosis (Figure 7C and Supplemental Video S10).

The torus experiment is a somewhat more rigorous test than a geometrically simple cell with parallel spindles, for example, which arise after a cytokinesis failure (Salmon and Wolniak, 1990; Argiros *et al.*, 2012), because the torus experiment excludes the possibility that spatial information derived from the previously failed cytokinesis may remain to contribute, positively or negatively, to specification of the secondary furrow. It also physically occludes the primary from the secondary zone, whereas these are continuous in a geometrically simple binucleate cell. However, in both cases, the cell contains spindles, chromosomes, and, as events proceed, nuclei. We therefore created anucleate, centrosome-containing cytoplasts from sand dollar or starfish embryos expressing either labeled wt or mutant Ect2 or Cyk4. This was accomplished by cutting metaphase cells with a glass needle passing between one pole and the rest of the mitotic apparatus. We used labeled histones or Hoechst 33342 to verify the absence of chromosomes from cytoplasts. After a small delay, the centrosome-containing cytoplast begins cyclical centrosome duplication. Although cytoplasts made from normal cells generate furrows at respectable frequency (von Dassow *et al.*, 2009), we found it impossible, despite numerous attempts, to achieve reliable furrowing from cytoplasts expressing excess wt or mutant Ect2. In the absence of a spindle or nuclei, exogenous wt Ect2 associated with the cortex and caused excessive contractility, whereas GEF-defective mutants strongly inhibited furrowing by cytoplasts. In a few out of very many cases, we detected wt or GEF4A Ect2 faintly in the overlap region between asters or associated with ingressing furrows (unpublished data). Cytoplasts from starfish embryos expressing exogenous Cyk4 had no such difficulties, however, and cleaved to completion consistently. Cyk4 unambiguously recruited to overlapping astral microtubules between pairs of centrosomes, concentrated beneath the "equatorial" cortex, and was gathered by the ingressing furrow into a midbody (Figure 8 and Supplemental Video S11). Cyk4-expressing cytoplasts from sand dollar embryos

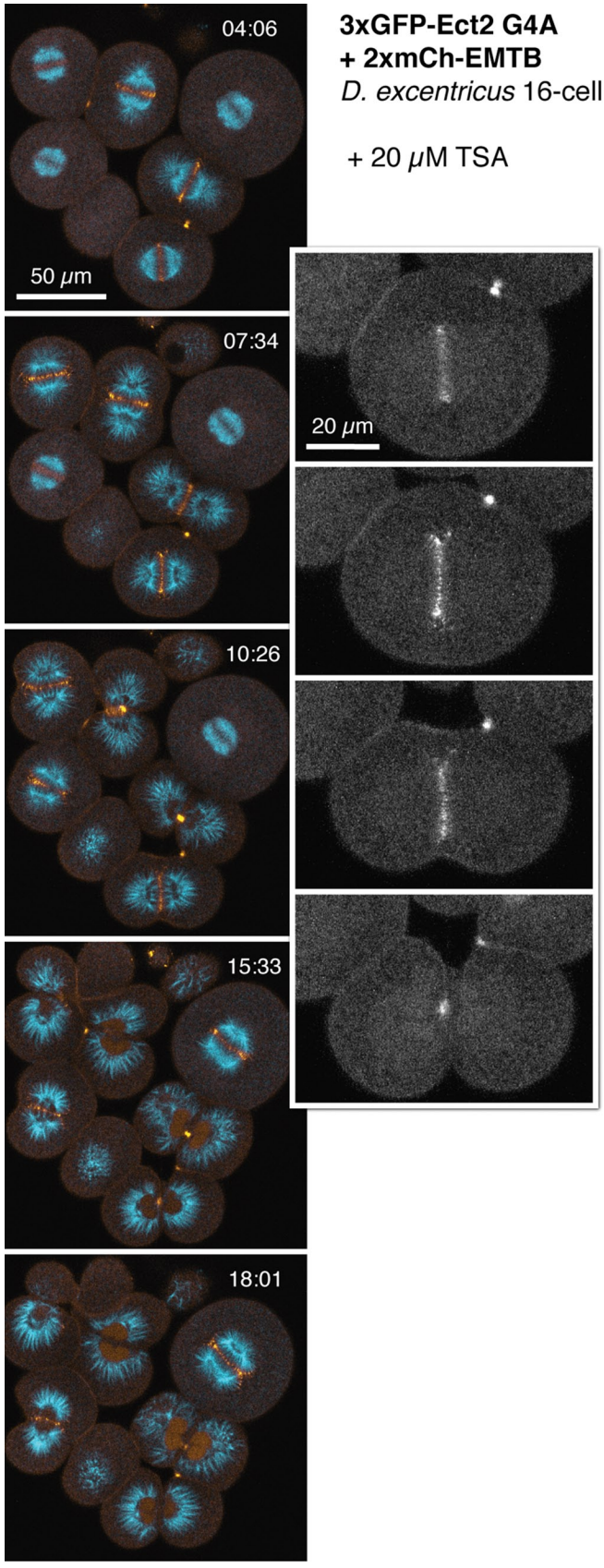

FIGURE 6: Sand dollar embryo expressing 3xGFP Ect2 GEF4A (gold) and 2xCh EMTB (blue) and treated with 20 μM trichostatin A at time 00:00 (minutes:seconds); projection of four 1-μm sections. Inset, 2× magnification of region covering the lowermost cell, Ect2 only.

similarly concentrated Cyk4 into midbodies (unpublished data), although with far lower expression level.

DISCUSSION

Our successful visualization of Ect2 and Cyk4 in live echinoderm embryos resolves a set of closely entwined, outstanding issues—whether there is a plausible means for astral microtubules to accomplish the same cytoplasmic patterning function as the spindle midzone; whether large cells likely use the same signaling mechanism as small cells for cytokinetic pattern formation; and whether multiple signaling pathways are required to account for classical experiments on embryonic cleavage. Meanwhile, an incidental but important finding of this study definitively narrows the set of possible physiological mechanisms for cytokinetic pattern formation. We discuss this first.

Current evidence strongly suggests that, in all animal cells, a zone of active Rho in the equatorial cortex is required for and directly prefigures assembly of the cytokinetic apparatus (Bement *et al.*, 2005; Yüce *et al.*, 2005; Motegi *et al.*, 2006; Nishimura and Yonemura, 2006). Specifically, the spatial domain of Rho activation is closely related to the zone of myosin recruitment (Yüce *et al.*, 2005; Foe and von Dassow, 2008). These spatial patterns scale with cell size, a fact that demands explanation (Bement *et al.*, 2005, 2006). Our analysis, in this study, of a Rho reporter in the context of overexpression of wild-type or dominant-negative Ect2 suggests that the amount of Rho activated is proportional to Ect2 activity. Although the available probes prevent us from visualizing both together, we found that all visible Ect2 is confined to the cell midplane—that is, the cytoplasmic disk containing both the spindle midzone and the equatorial cortex—at levels for which the Rho zone remains equatorially confined. Higher levels of wild-type Ect2 expression, at which we begin to detect labeled Ect2 on the cortex outside the equator, correspond to ectopic Rho activation outside the equator and concomitant cortical hyperactivity. Finally, a deregulated form of Ect2 (the C-terminal half lacking the BRCT domains) elicits nonpatterned Rho activation throughout the cortex, to levels vastly exceeding the total level of activity detected in normal cells. Regardless of the details, this finding substantially narrows the spectrum of possible explanations for the scaling of cytokinetic pattern formation by showing that the pool of available Rho is nonlimiting and indeed that no other generic factors significantly limit how much or over what area the cell can simultaneously activate Rho.

Meanwhile, we show definitively that both centralspindlin (as represented by the Cyk4 constituent) and Ect2 associate prominently with astral microtubules. Ever since the first articles describing the role of these proteins in cytokinesis, numerous diagrams (e.g., Somers and Saint, 2003) have expressed the hypothesis that they associate with astral microtubules, especially when oriented toward each other, just as well as with the central spindle. This hypothesis has even been expressed formally in an individual-based simulation in which the essential features are chosen to apply to echinoderm embryonic cells (Odell and Foe, 2008). Nonetheless, clear images that distinguish between spindle and aster have been elusive. In many cultured cell types, there is little room to make this distinction, although some exceptional studies succeeded for centralspindlin (e.g., Nishimura and Yonemura, 2006, show high-magnification images of centralspindlin on astral microtubule ends that are clearly distinct from the spindle). For large embryonic cells, outside of *C. elegans* embryos (in which furrow induction may indeed depend on additional cues; Dechant and Glotzer, 2003; Bringmann *et al.*, 2007; Tse *et al.*, 2012), few have looked. One notable study, using exceptionally careful fixation and an MKLP1 antibody, unambiguously showed centralspindlin on crossed astral microtubules in urchin embryos (Argiros *et al.*, 2012). To this we add the corresponding live visualization using labeled Cyk4, as well as what we believe to be the first live-cell documentation of Ect2 on the same population.

Furthermore, the concentration of centralspindlin, Ect2, and other participants at the midzone, combined with the demonstrated existence of an equatorially directed population of stable microtubules (Canman *et al.*, 2003; Foe and von Dassow, 2008), makes it plausible to hypothesize a unique signaling nexus operating at the midzone that may not be available elsewhere in the cell. In this study, however, we obtained numerous images in which both Cyk4 and Ect2 clearly associate with astral microtubules in the equatorial disk (i.e., between the midzone and the cortex) that are tens of micrometers from the spindle. In addition, and equally important, Cyk4 transiently decorates astral microtubules throughout the cell, appearing as it does so to vacate the aster center. Both features were evident whether or not the "cell" contained a proper spindle. Of note, in movies of both normal cells and anucleate cytoplasts or on the far side of toroidal cells, the association of Cyk4 with astral microtubules was absent in metaphase and then present shortly after anaphase. Taken together, these observations suggest that, as proposed previously (Hutterer *et al.*, 2009; Douglas *et al.*, 2010), centralspindlin can associate with any available microtubule in the cell but only after anaphase onset; that it accumulates in zones of overlap between directionally uniform microtubule arrays; and that, having accumulated, it recruits and activates a limited amount of Ect2. Thus, the microtubules of the spindle midzone, equatorial astral microtubules above a midzone, and juxtaposed asters without a midzone at all would each accomplish the same geometric condition with respect to Ect2 recruitment.

Finally, one of the primary motivations for this study was to resolve the apparent disagreement between classical micromanipulation studies on large echinoderm embryonic cells and modern molecular genetic studies on small cells and *C. elegans* embryos. The classical studies of Rappaport and Hiramoto (e.g., Rappaport, 1961; Hiramoto, 1971) purport to show spindle-independent induction of furrows by asters alone. In an extreme example, Hiramoto (1971) removed the spindle from a cell with a furrow underway and reported that the cell continued to cleave. Although these seminal works long remained the singular edifice of a few workers, most of the central findings have now been reproduced in urchin embryos (Shuster and Burgess, 2002; Bement *et al.*, 2005; von Dassow *et al.*, 2009) or other cells (e.g., Rieder *et al.*, 1997; Bringmann and Hyman, 2005; Baruni *et al.*, 2008), so they cannot be dismissed as either errors or species-specific anomalies. Nonetheless, the contrast with modern studies could not be more stark: time and again, the spindle midzone is shown to be the essential locus of cytokinetic signaling; time and again, both forward and reverse genetics associate this function with gene products whose visible localization in the cell also points to the midzone (Cao and Wang, 1996; Wheatley and Wang, 1996; Adams *et al.*, 1998; Jantsch-Plunger *et al.*, 2000; Somers and Saint, 2003; Yüce *et al.*, 2005). It is a formal possibility, even a likelihood, that cells use other cues for furrow induction, perhaps assessing concurrence between them to make cytokinetic patterning robust to mechanical perturbations. However, with rare exceptions (e.g., Bringmann *et al.*, 2007; Tse *et al.*, 2012), hypothetical midzone-independent cues have eluded genetics.

What we contribute to this dilemma is to show that the midzone-associated signaling ensemble is present in the right place and at the right time to account for cytokinetic furrow induction by juxtaposition of two asters. We find this to be the case whether the cell contains chromosomes and a functional spindle or not. A previous

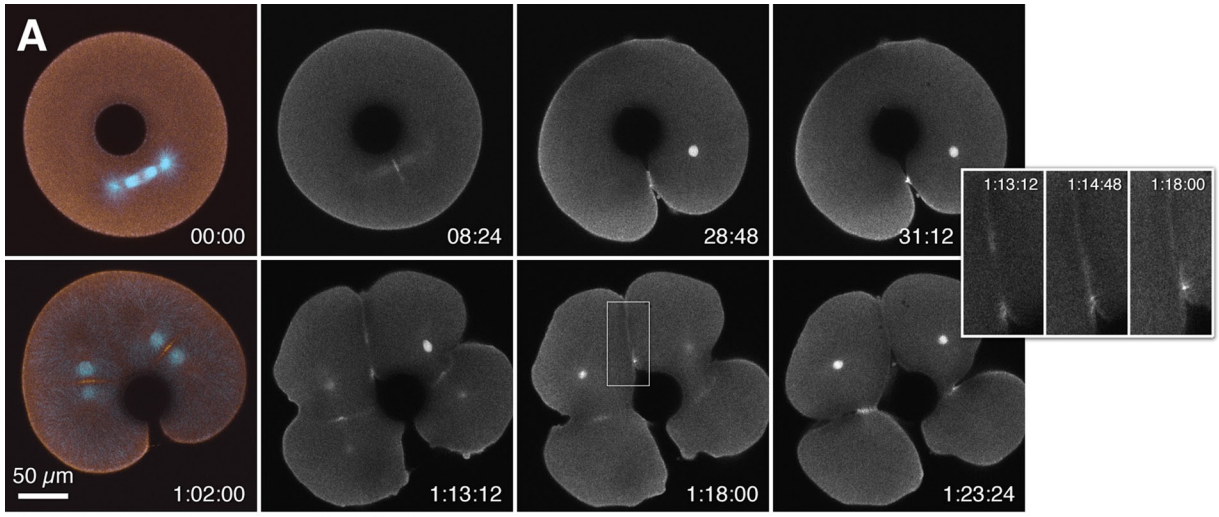

3xGFP-SpEct2 wt, 2xmCh-EMTB
P. miniata zygote

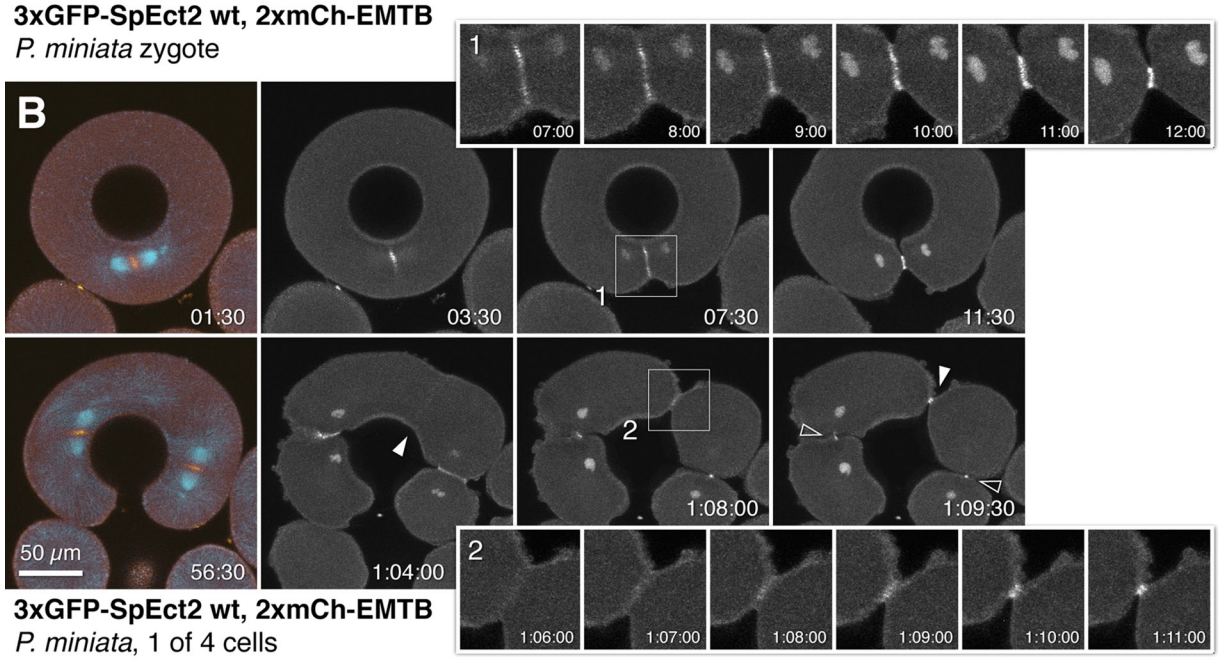

3xGFP-SpEct2 wt, 2xmCh-EMTB
P. miniata, 1 of 4 cells

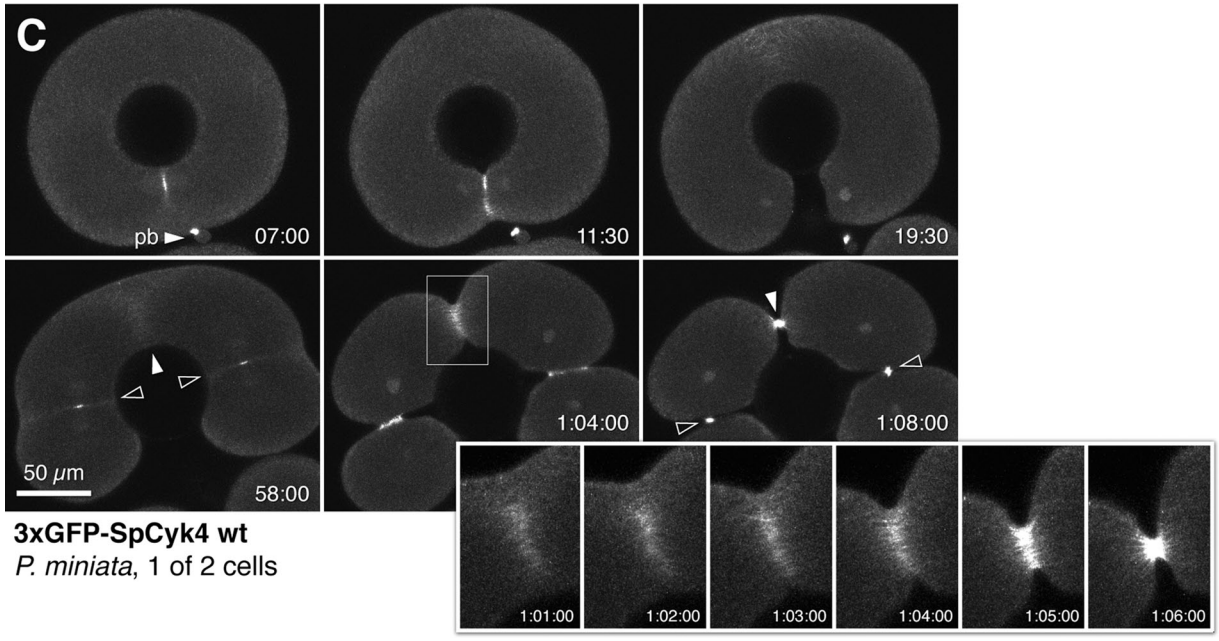

3xGFP-SpCyk4 wt
P. miniata, 1 of 2 cells

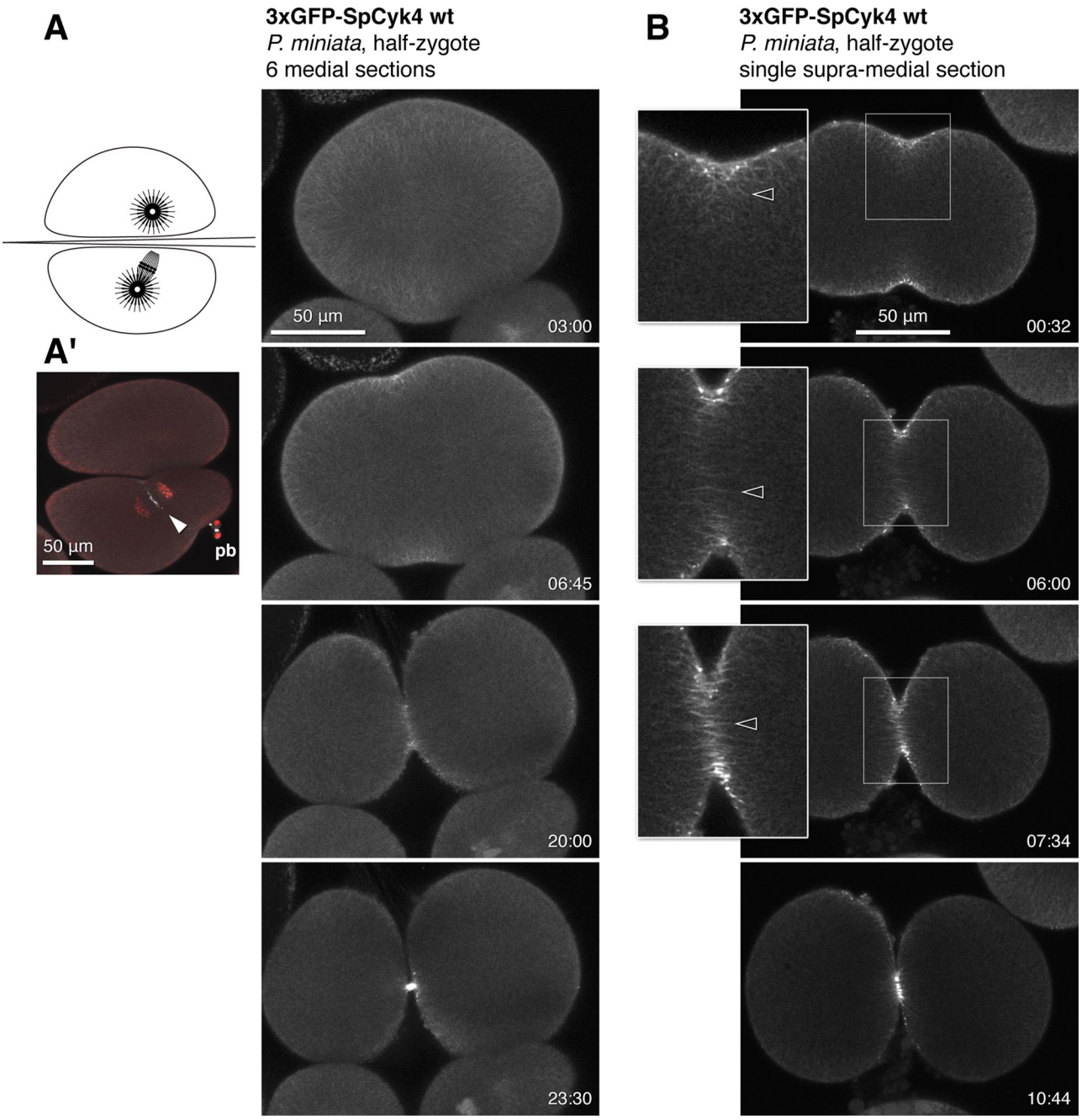

FIGURE 8: Centralspindlin recruits between paired asters in anucleate cytoplasts. Both panels show anucleate cytoplasts the first time they try to divide with two asters. (A) Medial view, projection of six sections; diagram depicts the operation. (A′) First cleavage of nucleate half of zygote in A (pb, polar bodies). (B) Single supramedial section; insets, 2× magnifications of boxed region; open arrows indicate astral microtubules decorated with Cyk4. See Supplemental Video S11.

study addressing this same topic, using antibody staining for MKLP1, in cells rendered binucleate by induced cleavage failure did not detect centralspindlin (or the chromosome passenger complex) between asters unless chromosomes became trapped between them (Argiros *et al.*, 2012). Mundane technical reasons likely do not account for this difference in results because we similarly found that in binucleate cells resulting from cleavage failure, Ect2 and Cyk4 are less likely to accumulate, and furrows less likely to ingress, between

FIGURE 7: Ect2 and centralspindlin are associated with secondary furrows in toroidal cells. Starfish zygote (A) and one of four cells (B) expressing wt 3xGFP Ect2 (gold) and 2xmCh EMTB (cyan) and perforated with a 50-µm glass bead (Supplemental Video S9). Top, first division after perforation; bottom, next division of resulting binucleate, U-shaped cell. Inset in A, 2× magnification of the secondary furrow region (boxed); insets 1 and 2 in B, primary and secondary furrows. (C) One of two cells in a starfish embryo expressing wt 3xGFP Cyk4 and perforated as in A and B (Supplemental Video S10); inset, secondary furrow region. Open arrowheads mark primary (spindle-crossing) furrows; solid arrowheads mark secondary furrows that pass between two asters.

cousin centrosomes than between sisters (Figure 3B; von Dassow and Bement, unpublished data). Instead, we suggest that the most interesting plausible reason for this discrepancy is that perhaps a chromosome-containing midzone is an effective competitor for a limited supply of potent signaling components, as suggested in *C. elegans* embryos (Baruni *et al.*, 2008). For this reason, we argue that the torus experiment and anucleate cytoplasts are more definitive: they positively associate Cyk4 and Ect2 accumulation with aster-dependent furrows. These experiments cannot exclude the existence of other signals for furrow induction, such as the polar astral inhibition signal (Bringmann and Hyman, 2005; Motegi *et al.*, 2006; Tse *et al.*, 2012; Zanin *et al.*, 2013), but our results show that either such signals are not required in echinoderm embryonic cells or they work by focusing centralspindlin on equatorially directed microtubules. Regardless, our results show that, rather than induce a furrow by some Cyk4- and Ect2-independent mechanism, the juxtaposition of spindle-less asters recreates the essential condition of the central spindle—closely apposed, oppositely oriented microtubules—even when, as in anucleate cytoplasts, there is none of the chromosome-associated information that likely contributes to spindle formation and centralspindlin recruitment under normal circumstances.

MATERIALS AND METHODS

Animals, gametes, and cells

The purple urchin, *Strongylocentrotus purpuratus*, was collected intertidally from South Cove at Cape Arago, Oregon. The sand dollar, *Dendraster excentricus*, was obtained by dredging in 5–10 fathoms off the North Spit, Coos Bay, Oregon. The bat star, *Patiria miniata*, was purchased from Marinus Scientific (Long Beach, CA). Animals were maintained in flowing natural seawater at the Oregon Institute of Marine Biology. Gametes of *S. purpuratus* and *D. excentricus* were obtained either by intracoelomic injection of 0.56 M KCl or, for purple urchins, by alternately bouncing and then shaking a gravid individual in the palm of the hand. Sperm were collected dry from the aboral surface and kept chilled until use. Purple urchin eggs were shed into a large volume of filtered seawater (FSW), rinsed twice in FSW, and stored settled at sea-table temperature (11–14°C) until use. Sand dollar eggs were shed into a large volume of FSW and left unrinsed at sea-table temperature until use. All echinoderm embryo culture likewise took place at sea-table temperature. Ovaries and testes of *P. miniata* were excised through a hole in the aboral epidermis made with a 4- or 5-mm biopsy punch; ovary fragments were washed in calcium-free artificial seawater (CFSW) and stored at 4–6°C before use, whereas testis were kept as close to dry as possible. Defolliculated immature oocytes were obtained by teasing apart ovary fragments and rinsing several times in CFSW and were then incubated in Millipore-filtered seawater (MFSW) at sea-table temperature for ~30 min before injection. Batches of oocytes with spontaneous maturation rates >~25% were discarded. A HeLa cell line stably expressing AcGFP-hEct2 was obtained from the previous study (Su *et al.*, 2011).

Egg handling

Purple urchin eggs were prepared for injection by dejellying with two rapid washes in calcium/magnesium-free artificial seawater and then returned to FSW in dishes rendered nonsticky by washing with 1% bovine serum albumin (BSA) in MFSW. Dejellied eggs were used within 1 h. For injections, coverslip-bottom dishes (MatTek, Ashland, MA) were coated by washing for 30 s in 1% protamine sulfate in distilled water, rinsing 3× in distilled water, and air drying. Dejellied purple urchin eggs were arranged under control of a mouth pipette in an injection dish filled with MFSW + 1 mM 3-aminotriazole to prevent hardening of the vitelline envelope and then fertilized before injection by addition of several drops of ~1:10,000 dilution of dry sperm. Good batches of gametes yield >90% fertilization within 5 min. For imaging, purple urchin embryos were removed from their still-soft vitelline envelopes using a hand-pulled mouth pipette and transferred either directly to a microscope slide or into a plastic Petri dish coated with 1% BSA in FSW.

Sand dollar eggs were fertilized within their jelly in a large volume of FSW by the addition of 1–2 ml of sperm diluted 1:10,000 in FSW. At 10–15 min after insemination, fertilized eggs were stripped of jelly and vitelline envelopes by a single passage in and out of a hand-pulled mouth pipette cut to slightly larger than the egg diameter. To prevent stripped eggs from sticking to glass, culture vessels were coated with 1% BSA in FSW. For injection, stripped sand dollar eggs were arranged by mouth pipette in an uncoated coverslip-bottom dish that had been cleaned with 95% ethanol. This treatment renders glass sticky enough to enable microinjection but allows damage-free release of injected embryos with gentle agitation.

Immediately before injection, defolliculated starfish oocytes were repeatedly sheared up and down by mouth pipette to disperse mucus and then arranged by mouth pipette into coverslip-bottomed injection dishes coated with protamine sulfate. Injected oocytes were cultured at sea-table temperature overnight or for as long as 2 d before use. Maturation was induced in small batches by addition of 10^{-6}–10^{-5} M 1-methyladenine in distilled water. After germinal vesicle breakdown (45–60 min), eggs were inseminated by careful addition of dilute sperm suspension by mouth pipette while observing under a microscope to gauge sperm motility and engagement. This proved important because oocytes so handled are often susceptible to polyspermy when inseminated in bulk. If required, fertilized starfish eggs were stripped of the fertilization envelope by transferring them to dishes coated with a layer of 1% agar in seawater and filled with seawater in which had been freshly dissolved 1% sodium thioglycolate titrated to pH 9.5 by addition of 1 M KOH. Eggs were observed continuously as the membrane thinned, stripped by gently shearing with a mouth pipette, and then rinsed three times through MFSW and cultured in agar-coated dishes.

Injections and micromanipulation

All injections were conducted on an inverted microscope at a temperature of 18–20°C using a Narishige (East Meadow, NY) oil-hydraulic manipulator and pressure injector (Dagan, Minneapolis, MN), using glass needles crafted from 1-mm–outer diameter filament-containing capillaries (Sutter, Novato, CA) by a P-97 Flaming-Brown puller (Sutter) and silanized by hexamethyldisilazane vapor, then filled and broken against a glass edge to a diameter of 2–5 µm. Purple urchins and sand dollars were typically injected with puffs corresponding to 2–3% of cytoplasmic volume and starfish oocytes to <1%, avoiding the germinal vesicle (a purple urchin egg is 75–80 µm in diameter, ~0.25 nl; a sand dollar egg is 125–130 µm, ~1 nl; and a starfish egg is 180–200 µm, ~4 nl). mRNA dissolved in nuclease-free water was injected at concentration ranges as follows: 3xGFP and 3xmCh SpEct2wt, 25–100 ng/µl; 3xGFP SpEct2 GEF4A, 100–200 ng/µl; 3xGFP SpEct2 GEFV560A, 250 ng/µl; SpEct2CT, 50–180 ng/µl; 3xGFP SpCyk4, 100 ng/µl; mCh-H2B, 50-100 ng/µl; eGFP-rGBD, 250–1000 ng/µl; and 2xmCh EMTB, 100–300 ng/µl. To induce strong cytokinetic defects (Figure 2), wt SpEct2 and SpEct2 GEF4A were injected at 250 ng/µl.

To generate anucleate cytoplasts, fertilized eggs deprived of their various envelopes were arranged in coverslip-bottom dishes, either soon after injection (for sand dollars and purple urchins) or

after completion of meiosis (for starfish), and then bisected with an injection needle held either by hand or in an oil hydraulic manipulator. In all such experiments, cut fragments were either stained with Hoechst 33342 (~10 ng/ml) or expressed labeled histone H2B; this allowed us to verify that all chromosomes had been segregated to one side of the cut. To perforate eggs, we used a Narishige MF-830 microforge to shape an injection needle, melting a bead of measured size and then introducing a 45–60° bend in the stem such that the tool, when held at 30°, could be lowered nearly straight down upon a cell using an oil-hydraulic micromanipulator mounted on the stage of the confocal.

Constructs and mRNA synthesis

S. purpuratus Ect2 (SpEct2) was amplified from zygote cDNA using primers (5′-GGTTCCGGAACCATGGCAGCGCCCATGGAAGTAACAG-3′ and 5′-GAGCTCGAGTCAAAGCTTTTTGCTGGCTGATGGT-3′) introducing *Bsp*EI/*Xho*I restriction sites (underlined) and inserted into pCS2-3xGFP/mCherry vector (von Dassow *et al.*, 2009) to generate fusions at the Ect2 N-terminus. The domain organization and sequence of SpEct2 were highly similar to those of human Ect2 (Figure 1A). Constructs of Ect2-CT (396-883AA), GEFV560A, and GEF4A (559-562 PVQR>AAAA) were created using PCR (Phusion High-Fidelity DNA Polymerase; Finnzymes, Pittsburgh, PA). mRNA for various SpEct2-derived constructs, 3xGFP SpCyk4 (Clark *et al.*, 2012), 2xmCh EMTB (von Dassow *et al.*, 2009), and eGFP-rGBD (Benink and Bement, 2005) was transcribed using SP6 mMessage mMachine kit (Applied Biosystems, Grand Island, NY) according to the manufacturer's instructions.

Microscopy

All imaging of echinoderm embryos was conducted on an Olympus (Center Valley, PA) FluoView 1000 laser-scanning confocal on an IX81 inverted stand, using either a 60×/1.2 numerical aperture (NA) or a 40×/1.15 NA water-immersion objective. The stage was equipped with Peltier cooling adaptors (Dagan) set to 12–14°C (depending on current sea-table temperature). For filming live embryos, cells in MFSW were held between slide and coverslip; these were joined by ridges of high-vacuum grease (Dow Corning, Midland, MI) and compressed to the point at which cells were just trapped, if necessary, or left uncompressed for realistic surface views. Volumes of seawater and numbers of embryos per preparation were limited to avoid anoxia. For surface views and to prevent cleavage abnormalities, glass surfaces were coated with 1% BSA in seawater the day of use. For some experiments (e.g., toroidal cells) embryos were imaged in coverslip-bottom dishes using a matching cooling stage.

HeLa AcGFP-hEct2 cells were imaged in phenol red–free, CO_2-independent medium supplemented with 20% fetal calf serum, 0.2 mM L-glutamine, antibiotics, and 1 mM Na pyruvate (all Invitrogen, Grand Island, NY) using the Perkin Elmer (Waltham, MA) ERS spinning disk system (Su *et al.*, 2011).

Image processing and analysis

Measurement of the width of the cell with corresponding Rho zone was carried out manually using FluoView software (Olympus). Subtraction of autofluorescent granules (Supplemental Figure S1A) was carried out in ImageJ (National Institutes of Health, Bethesda, MD) by subtracting the scaled square root of the product of the GFP and mCherry channels from the GFP channel. No convolution filters or other image processing, beyond adjustment of white and black points, brightest-point projection, and frame averaging as noted, was applied to any image; where necessary, false-color merges were prepared in Photoshop CS4 (Adobe, San Jose, CA), using color tables that preserve luminosity. Kymographs were prepared using ImageJ.

ACKNOWLEDGMENTS

We thank Brittney Dlouhy-Massengale for technical help and Sveta Maslakova for hosting us in her lab. This work was supported by National Science Foundation Grants MCB-0917887 and MCB-1041200 to G.vD., EMBO fellowship ASTF 245-2012 to K.C.S., and National Institutes of Health Grant GM52932 to W.M.B. Work in M.P.'s lab is supported by Cancer Research UK and the EMBO Young Investigator Programme.

REFERENCES

Adams RR, Tavares AA, Salzberg A, Bellen HJ, Glover DM (1998). pavarotti encodes a kinesin-like protein required to organize the central spindle and contractile ring for cytokinesis. Genes Dev 12, 1483–1494.

Argiros H, Henson L, Holguin C, Foe V, Shuster CB (2012). Centralspindlin and chromosomal passenger complex behavior during normal and Rappaport furrow specification in echinoderm embryos. Cytoskeleton (Hoboken) 69, 840–853.

Baruni JK, Munro EM, von Dassow G (2008). Cytokinetic furrowing in toroidal, binucleate and anucleate cells in C. elegans embryos. J Cell Sci 121, 306–316.

Bement WM, Benink HA, von Dassow G (2005). A microtubule-dependent zone of active RhoA during cleavage plane specification. J Cell Biol 170, 91–101.

Bement WM, Miller AL, von Dassow G (2006). Rho GTPase activity zones and transient contractile arrays. Bioessays 28, 983–993.

Benink HA, Bement WM (2005). Concentric zones of active RhoA and Cdc42 around single cell wounds. J Cell Biol 168, 429–439.

Bringmann H, Cowan CR, Kong J, Hyman AA (2007). LET-99, GOA-1/GPA-16, and GPR-1/2 are required for aster-positioned cytokinesis. Curr Biol 17, 185–191.

Bringmann H, Hyman AA (2005). A cytokinesis furrow is positioned by two consecutive signals. Nature 436, 731–734.

Canman JC, Cameron LA, Maddox PS, Straight A, Tirnauer JS, Mitchison TJ, Fang G, Kapoor TM, Salmon ED (2003). Determining the position of the cell division plane. Nature 424, 1074–1078.

Canman JC, Hoffman DB, Salmon ED (2000). The role of pre- and post-anaphase microtubules in the cytokinesis phase of the cell cycle. Curr Biol 10, 611–614.

Cao LG, Wang YL (1996). Signals from the spindle midzone are required for the stimulation of cytokinesis in cultured epithelial cells. Mol Biol Cell 7, 225–232.

Chalamalasetty RB, Hümmer S, Nigg EA, Silljé HH (2006). Influence of human Ect2 depletion and overexpression on cleavage furrow formation and abscission. J Cell Sci 119, 3008–3019.

Clark AG, Sider JR, Verbrugghe K, Fenteany G, von Dassow G, Bement WM (2012). Identification of small molecule inhibitors of cytokinesis and single cell wound repair. Cytoskeleton (Hoboken) 69, 1010–1020.

Dechant R, Glotzer M (2003). Centrosome separation and central spindle assembly act in redundant pathways that regulate microtubule density and trigger cleavage furrow formation. Dev Cell 4, 333–344.

Douglas ME, Davies T, Joseph N, Mishima M (2010). Aurora B and 14–3-3 coordinately regulate clustering of centralspindlin during cytokinesis. Curr Biol 20, 927–933.

Eckley DM, Ainsztein AM, Mackay AM, Goldberg IG, Earnshaw WC (1997). Chromosomal proteins and cytokinesis: patterns of cleavage furrow formation and inner centromere protein positioning in mitotic heterokaryons and mid-anaphase cells. J Cell Biol 136, 1169–1183.

Foe VE, von Dassow G (2008). Stable and dynamic microtubules coordinately shape the myosin activation zone during cytokinetic furrow formation. J Cell Biol 183, 457–470.

Green RA, Paluch E, Oegema K (2012). Cytokinesis in animal cells. Annu Rev Cell Dev Biol 28, 29–58.

Hiramoto Y (1971). Analysis of cleavage stimulus by means of micromanipulation of sea urchin eggs. Exp Cell Res 68, 291–298.

Hutterer A, Glotzer M, Mishima M (2009). Clustering of centralspindlin is essential for its accumulation to the central spindle and the midbody. Curr Biol 19, 2043–2049.

Jantsch-Plunger V, Gonczy P, Romano A, Schnabel H, Hamill D, Schnabel R, Hyman AA, Glotzer M (2000). CYK-4: A Rho family gtpase activating

protein (GAP) required for central spindle formation and cytokinesis. J Cell Biol 149, 1391–1404.
Lekomtsev S, Su KC, Pye VE, Blight K, Sundaramoorthy S, Takaki T, Collinson LM, Cherepanov P, Divecha N, Petronczki M (2012). Centralspindlin links the mitotic spindle to the plasma membrane during cytokinesis. Nature 492, 276–279.
Liu X, Wang H, Eberstadt M, Schnuchel A, Olejniczak ET, Meadows RP, Schkeryantz JM, Janowick DA, Harlan JE, Harris EA, *et al*. (1998). NMR structure and mutagenesis of the N-terminal Dbl homology domain of the nucleotide exchange factor Trio. Cell 95, 269–277.
Mishima M, Kaitna S, Glotzer M (2002). Central spindle assembly and cytokinesis require a kinesin-like protein/RhoGAP complex with microtubule bundling activity. Dev Cell 2, 41–54.
Motegi F, Velarde NV, Piano F, Sugimoto A (2006). Two phases of astral microtubule activity during cytokinesis in C. elegans embryos. Dev Cell 10, 509–520.
Murata-Hori M, Wang YL (2002). Both midzone and astral microtubules are involved in the delivery of cytokinesis signals: insights from the mobility of aurora B. J Cell Biol 159, 45–53.
Nishimura Y, Yonemura S (2006). Centralspindlin regulates ECT2 and RhoA accumulation at the equatorial cortex during cytokinesis. J. Cell Sci 119, 104–114.
Nislow C, Lombillo VA, Kuriyama R, McIntosh JR (1992). A plus-end-directed motor enzyme that moves antiparallel microtubules in vitro localizes to the interzone of mitotic spindles. Nature 359, 543–547.
Odell GM, Foe VE (2008). An agent-based model contrasts opposite effects of dynamic and stable microtubules on cleavage furrow positioning. J Cell Biol 183, 471–483.
Prokopenko SN, Brumby A, O'Keefe L, Prior L, He Y, Saint R, Bellen HJ (1999). A putative exchange factor for Rho1 GTPase is required for initiation of cytokinesis in Drosophila. Genes Dev 13, 2301–2314.
Rappaport R (1961). Experiments concerning the cleavage stimulus in sand dollar eggs. J Exp Zool 148, 81–89.
Rappaport R (1996). Cytokinesis in Animal Cells, Cambridge, UK: Cambridge University Press.
Rieder CL, Khodjakov A, Paliulis LV, Fortier TM, Cole RW, Sluder G (1997). Mitosis in vertebrate somatic cells with two spindles: implications for the metaphase/anaphase transition checkpoint and cleavage. Proc Natl Acad Sci USA 94, 5107–5112.
Salmon ED, Wolniak SM (1990). Role of microtubules in stimulating cytokinesis in animal cells. Ann NY Acad Sci 582, 88–98.
Schumacher S, Gryzik T, Tannebaum S, Müller HA (2004). The RhoGEF Pebble is required for cell shape changes during cell migration triggered by the Drosophila FGF receptor Heartless. Development 131, 2631–2640.
Shuster CB, Burgess DR (2002). Transitions regulating the timing of cytokinesis in embryonic cells. Curr Biol 12, 854–858.
Somers WG, Saint R (2003). A RhoGEF and Rho family GTPase-activating protein complex links the contractile ring to cortical microtubules at the onset of cytokinesis. Dev Cell 4, 29–39.
Su KC, Takaki T, Petronczki M (2011). Targeting of the RhoGEF Ect2 to the equatorial membrane controls cleavage furrow formation during cytokinesis. Dev Cell 21, 1104–1115.
Tatsumoto T, Xie X, Blumenthal R, Okamoto I, Miki T (1999). Human ECT2 is an exchange factor for Rho GTPases, phosphorylated in G2/M phases, and involved in cytokinesis. J Cell Biol 147, 921–928.
Tse YC, Werner M, Longhini KM, Labbe JC, Goldstein B, Glotzer M (2012). RhoA activation during polarization and cytokinesis of the early Caenorhabditis elegans embryo is differentially dependent on NOP-1 and CYK-4. Mol Biol Cell 23, 4020–4031.
von Dassow G (2009). Concurrent cues for cytokinetic furrow induction in animal cells. Trends Cell Biol 19, 165–173.
von Dassow G, Verbrugghe KJ, Miller AL, Sider JR, Bement WM (2009). Action at a distance during cytokinesis. J Cell Biol 187, 831–845.
Werner M, Munro E, Glotzer M (2007). Astral signals spatially bias cortical myosin recruitment to break symmetry and promote cytokinesis. Curr Biol 17, 1286–1297.
Wheatley SP, Wang YL (1996). Midzone microtubule bundles are continuously required for cytokinesis in cultured epithelial cells. J Cell Biol 135, 981–989.
White EA, Glotzer M (2012). Centralspindlin: at the heart of cytokinesis. Cytoskeleton (Hoboken) 69, 882–892.
Yüce O, Piekny A, Glotzer M (2005). An ECT2-centralspindlin complex regulates the localization and function of RhoA. J Cell Biol 170, 571–582.
Zanin E, Desai A, Poser I, Toyoda Y, Andree C, Moebius C, Bickle M, Conradt B, Piekny A, Oegema K (2013). A conserved RhoGAP limits M phase contractility and coordinates with microtubule asters to confine RhoA during cytokinesis. Dev Cell 26, 496–510.